Circulating Histones Are Mediators of Trauma-associated Lung Injury

Simon T. Abrams[1,2]*, Nan Zhang[3]*, Joanna Manson[4], Tingting Liu[2], Caroline Dart[5], Florence Baluwa[2], Susan Siyu Wang[6], Karim Brohi[4], Anja Kipar[7], Weiping Yu[3], Guozheng Wang[2], and Cheng-Hock Toh[1,2]

[1]National Institute of Health Research Biomedical Research Centre, Royal Liverpool University Hospital and [2]Institute of Infection and Global Health, University of Liverpool, Liverpool, United Kingdom; [3]Medical School, Southeast University, Nanjing, China; [4]Trauma Sciences, Barts and the London School of Medicine and Dentistry, Queen Mary University of London, London, United Kingdom; [5]Institute of Integrative Biology, University of Liverpool, Liverpool, United Kingdom; [6]School of Clinical Medicine, University of Cambridge, Cambridge, United Kingdom; and [7]Veterinary Pathology, School of Veterinary Science, University of Liverpool, Liverpool, United Kingdom

***Rationale*: Acute lung injury is a common complication after severe trauma, which predisposes patients to multiple organ failure. This syndrome largely accounts for the late mortality that arises and despite many theories, the pathological mechanism is not fully understood. Discovery of histone-induced toxicity in mice presents a new dimension for elucidating the underlying pathophysiology.**

***Objectives*: To investigate the pathological roles of circulating histones in trauma-induced lung injury.**

***Methods*: Circulating histone levels in patients with severe trauma were determined and correlated with respiratory failure and Sequential Organ Failure Assessment (SOFA) scores. Their cause–effect relationship was studied using cells and mouse models.**

***Measurements and Main Results*: In a cohort of 52 patients with severe nonthoracic blunt trauma, circulating histones surged immediately after trauma to levels that were toxic to cultured endothelial cells. The high levels were significantly associated with the incidence of acute lung injury and SOFA scores, as well as markers of endothelial damage and coagulation activation. In *in vitro* systems, histones damaged endothelial cells, stimulated cytokine release, and induced neutrophil extracellular trap formation and myeloperoxidase release. Cellular toxicity resulted from their direct membrane interaction and resultant calcium influx. In mouse models, cytokines and markers for endothelial damage and coagulation activation significantly increased immediately after trauma or histone infusion. Pathological examinations showed that lungs were the predominantly affected organ with edema, hemorrhage, microvascular thrombosis, and neutrophil congestion. An anti-histone antibody could reduce these changes and protect mice from histone-induced lethality.**

***Conclusions*: This study elucidates a new mechanism for acute lung injury after severe trauma and proposes that circulating histones are viable therapeutic targets for improving survival outcomes in patients.**

AT A GLANCE COMMENTARY

Scientific Knowledge on the Subject

Acute lung injury is a common complication of severe trauma that may lead to multiple organ failure. This failure is a major cause of late death, but the underlying mechanism is poorly understood.

What This Study Adds to the Field

This study demonstrates a new mechanism of acute lung injury caused by severe nonthoracic blunt trauma. In these patients, circulating histones rise to toxic levels and serve as mediators of distant organ damage, with the lungs being the most susceptible. Histone toxicity originates from their affinity for phosphate groups within DNA and phospholipids; interactions with the latter lead to their integration into cell membranes and cause large inward ion currents and calcium influx. This effect on insulted cells leads to endothelial damage, coagulation activation, cytokine release, and neutrophil extracellular trap formation. Discovery of these toxic effects highlights a cause of the major pathological changes in posttrauma lung injury.

Keywords: lung; trauma; histones

Trauma continues to result in more deaths during the first decades of life than all other diseases (1). Besides its immediately lethal effect, the high morbidity and mortality are largely through the development of multiple organ failure (MOF) (2, 3). Clinical presentation of MOF generally begins with respiratory failure followed by cardiovascular failure before other organs become affected (4). Furthermore, the severity of acute lung injury or dysfunction is strongly associated with the incidence of MOF (4). Postmortem findings also show the lungs to be more frequently affected than any other organ in patients who die of clinical shock or after trauma (5). The underlying pathological changes include neutrophil infiltration, pulmonary edema, hemorrhage, and microvascular thromboses (5).

Theories on pathogenesis have been based mainly on findings of a systemic inflammatory state from evidence of cytokine release and neutrophil activation (3, 6). The heightened elevation of proinflammatory cytokines has not been well explained because levels appear disproportionately high in the absence of infection. This has led to speculation that increased gut permeability could be facilitating bacterial translocation and endotoxemia (7, 8). However, such theories are incomplete in adequately explaining how lung injury occurs fairly soon after nonthoracic trauma, when the effects of cytokines or bacterial translocation would take

(*Received in original form June 9, 2012; accepted in final form October 21, 2012*)

* These authors contributed equally to the study.

Author Contributions: S.T.A. conducted and analyzed *in vitro* assays of histone toxicity and endothelial permeability as well as ELISA, liver/renal functions. N.Z. and W.Y. performed the animal experiments. T.L. produced ahscFv, cscFv, and human/mouse histones and undertook the Western blotting and immunohistochemical staining. F.B. undertook ELISA and immunohistochemical staining. S.S.W. conducted the *in vitro* endothelial permeability assay. C.D. performed the electrophysiology. A.K. undertook histological examinations. J.M. and K.B. collected human plasma and performed the nucleosome ELISA. G.W. designed and produced ahscFv and cscFv, planned and organized the project, and wrote the manuscript with C.-H.T. as overall supervisor.

Correspondence and requests for reprints should be addressed to Cheng-Hock Toh, M.D., National Institute of Health Research Biomedical Research Centre, Royal Liverpool University Hospital, Liverpool L7 8XP, UK. E-mail: toh@liv.ac.uk; or Guozheng Wang, M.D., Ph.D., Institute of Infection and Global Health, University of Liverpool, Liverpool L69 3GA, UK. E-mail: wangg@liv.ac.uk

This article has an online supplement, which is available from this issue's table of contents at www.atsjournals.org

Am J Respir Crit Care Med Vol 187, Iss. 2, pp 160–169, Jan 15, 2013

Originally Published in Press as DOI: 10.1164/rccm.201206-1037OC on December 6, 2012
Internet address: www.atsjournals.org

several hours. Furthermore, treatment strategies targeting cytokines, complement, and other mediators have been trialed without significant benefit (2). The current pathogenic understanding of trauma-associated MOF and respiratory failure *per se* is therefore incomplete.

Elevation of nuclear proteins after severe tissue injury has been reported, for example, HMGB1 (9), but the role played by histones, which are the major nuclear proteins, has not been examined. Chromatin is initially cleaved into oligo- and mononucleosomes before further degradation into individual histones. However, these components are rarely detectable unless there is extensive cell death (10) because of rapid hepatic clearance (11). Histone-induced endothelial damage (12), cytokine elevation (13, 14), platelet aggregation (15), and coagulation activation (15, 16) have been demonstrated in mouse models. These data add an important factor for understanding the pathogenesis of postinjury lung dysfunction and MOF. We hypothesize that circulating histones serve as direct mediators of distant organ damage leading on to MOF after predominant lung injury. To test this hypothesis, we have examined patients with severe nonthoracic blunt trauma to elucidate whether histones released after injury can be pathogenic. Underlying mechanisms and physiological relevance are further dissected through *in vitro* and *in vivo* experiments, including a mouse model of trauma. Some of the results of these studies has been previously reported in the form of an abstract (17).

METHODS

Patients

Patients with severe trauma were recruited as part of a prospective cohort study, Activation of Coagulation and Inflammation in Trauma, at the Royal London Hospital (London, UK), a major trauma center in the United Kingdom. Patient recruitment and sampling procedures with full ethical approval are described in the online supplement.

Animal Experiments

C57BL/6 male mice from the SLAC Experimental Animal Center (Shanghai, China) were housed and used under sterile conditions at the Research Center of Genetically Modified Mice (Southeast University, Nanjing, China). Ethical issues and detailed procedures are included in the online supplement.

Reagents

Recombinant histones from New England BioLabs (Herts, UK) and calf thymus histones from Roche (Indianapolis, IN) were purchased. Human and mouse histones were isolated from cultured U937 cells and mouse liver, respectively, as described previously (18). Anti-histone scFv (ahscFv) was designed on the basis of sequences of complementarity-determining regions (CDRs) of anti-histone antibodies from mice with autoimmune disorders (19). Control scFv (cscFv) was designed by replacing all the CDRs in ahscFv (*see* Figure E2A in the online supplement) and both were synthesized, subcloned into the PET16 vector, expressed in *Escherichia coli* BL21 (Novagen, Middlesex, UK), and purified with His-binding resin. LPS contamination was monitored with E-TOXATE reagents (Sigma, Dorset, UK).

In Vitro Histone Cytotoxicity Assay

Flow cytometric analysis of propidium iodide–stained damaged nuclei, as previously described (20), clearly separated damaged and viable cells (Figures E1A–E1C). Cell survival rates were normalized by untreated controls (designated as 100%).

Neutrophil Extracellular Trap Formation and Myeloperoxidase Release

Neutrophils were isolated using a Percoll (Sigma-Aldrich) gradient. After treatment, cells were fixed in 4% paraformaldehyde and stained with propidium iodide (10 μg/ml). Neutrophil extracellular trap (NETs) were visualized by confocal microscopy (LSM-710; Zeiss, Jena, Germany). Extracellular myeloperoxidase (MPO) activity was measured with an EnzChek myeloperoxidase activity assay kit (Invitrogen, Paisley, UK).

Immunohistochemical Staining

After antigen retrieval with the PT link for pre-treatment system (Dako, Glostrup, Denmark), paraffin-embedded sections were stained with anti–histone H3, anti–citrullinated (cit) histone H3, and anti-MPO (Abcam, Cambridge, UK), and with anti-fibrin and an EnVision kit (Dako). To confirm specificity, antibodies were either preincubated with specific antigen or secondary antibody alone as controls to validate each batch of staining. Images were visualized by microscopy (Olympus, Southend-on-Sea, UK) and recorded.

Permeability Assay

Permeability of a confluent endothelial monolayer was analyzed in a dual-chamber system using Evans blue–labeled bovine serum albumin, as previously described (21). Permeability changes *in vivo* involved assessing for pulmonary edema by measuring the wet-to-dry weight ratio of the right lung of mice, as previously described (22). Details are included in the online supplement.

Electrophysiology and Intracellular Calcium Measurement

Whole-cell currents were recorded in the perforated patch configuration from single EA.hy926 cells, using an Axopatch 200B amplifier (Axon Instruments, Inverurie, UK), as previously described (23). $[Ca^{2+}]_i$ was determined as described previously (24), using Fura-2AM as the fluorescent probe. Details are provided in the online supplement.

Statistical Analysis

Intergroup differences were analyzed by analysis of variance followed by the Student-Newman-Keuls test. Two-group comparisons were done by Student *t* test. Animal survival time was analyzed by a log-rank test and association used simple linear correlation. For patient data, a median test and Fisher exact test were used if data were not normally distributed.

RESULTS

Circulating Histones Reach Toxic Levels in Patients with Severe Blunt Trauma

The harmful effects of extracellular histones that have been reported have exclusively used exogenous histones. Although the presence of circulating nucleosomes in patients has been reported (25), there are no data describing the individual histones released after nucleosome degradation. In this study, we first investigated 250 patients with severe trauma and found that circulating nucleosome levels correlated positively with the injury severity scores (26) (Figure 1A). Longitudinal analysis showed nucleosomes reaching maximal levels (100%) within 4 hours with near complete clearance after 24 hours, whereas histones were elevated at 4 hours and peaked at about 24 hours with high levels still detectable at 72 hours after trauma in many cases (Figure 1B). Total nondegraded circulating histone levels ranged from 10 to 230 μg/ml within 4 hours of injury (median, 28.6 μg/ml; quartile: 13.7, 58.9), which was significantly higher than in healthy donors (n = 20) (median, 2.3 μg/ml; quartile: 0.5, 3.6) (Figure 1C). These data confirm that severely injured tissues release large quantities of nucleosomes into the circulation, which were further broken down into individual histones.

A previous report showed that exogenous histones are toxic to cultured mouse intestinal epithelial cells in serum-free medium, but lost toxicity in 10% fetal calf serum (27). Other

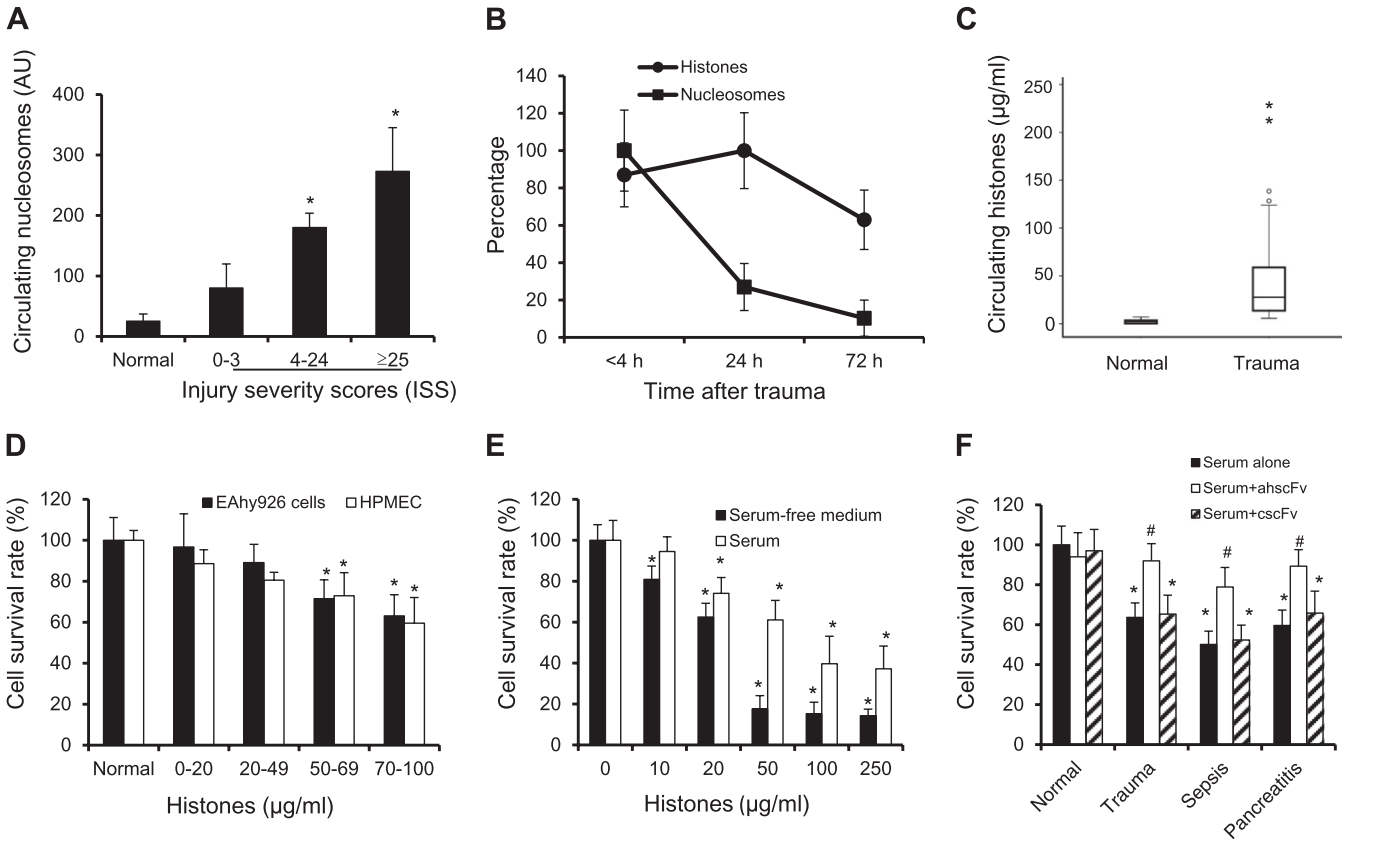

Figure 1. Extensive cell death in trauma patients elevates circulating histones to levels that damage endothelial cells *in vivo*. (*A*) Circulating nucleosome levels at admission in 250 trauma patients (Table E1) were detected by ELISA. The means ± SD in healthy donors (Normal, n = 20) and patients grouped by injury severity score (ISS) (0–3, n = 38; 4–24, n = 111; >25, n = 101; total, 250 patients) are presented. *Analysis of variance (ANOVA) test shows significant increases in patients with higher ISS compared with normal and low-ISS groups (0–3). (*B*) The dynamic change in circulating nucleosomes and histones in patients with severe trauma. Maximal values at a time point were set up as 100% and relative percentages are shown (means ± SD). (*C*) Box plot of total circulating histones in healthy donors and 52 patients with severe nonthoracic blunt trauma; median test, $P < 0.01$. (*D*) EA.hy926 cells and human pulmonary microvascular endothelial cells (HPMECs) were treated for 1 hour with serum from trauma patients on admission and the cell survival rate was measured (*see* METHODS). Survival rates (means ± SD) relative to that of healthy donor cells treated with serum (Normal, designated 100%) are presented. *ANOVA test shows a significant decrease compared with normal ($P < 0.05$). (*E*) EA.hy926 cells were incubated for 1 hour with serum-free medium or 80% human serum from three healthy donors supplemented with various concentrations of calf thymus histones. The normalized percentage of surviving cells (means ± SD) from three independent experiments are shown. *ANOVA test shows significant reduction compared with untreated cells ($P < 0.05$). Histone effect became significant at a concentration as low as 10 μg/ml in serum-free medium, and 20 μg/ml in serum. (*F*) EA.hy926 cells were treated with serum from healthy donors (Normal) or from patients with trauma, sepsis, or pancreatitis in the absence or presence of anti-histone scFv (ahscFv) or control scFv (cscFv) (200 μg/ml). Sera from patients containing histones at more than 50 μg/ml were selected and each group had at least three patients. *ANOVA test shows significant reduction in cell survival rates compared with normal ($P < 0.05$). #ANOVA test shows significant increase in cell survival rates in the presence of ahscFv compared with that without ahscFv or with cscFv ($P < 0.05$).

reports showed that histones only induced aggregation of washed platelets, but not of platelets in plasma (15, 28). These data suggest that circulating histones are nontoxic, which contradicts the fact that infusing histones into blood kills mice. To clarify this in a clinical context, we collected sera from patients and found that serum was toxic to cultured endothelial cells once histone levels exceeded 50 μg/ml (Figure 1D). Seventeen of 52 patients (32.7%) with severe blunt trauma had circulating histones exceeding this level. Using normal serum supplemented with calf thymus histones, we found a similar dose response (Figure 1E), except the toxicity became significant at 20 μg/ml. Isolated human and mouse histones showed toxicity profiles similar to that of calf thymus histones when incubated with various human endothelial cells or injected into mice (Figures E1D and E1E). These data suggest that histone toxicity is not species or cell type specific.

To confirm that the toxicity was due to histones in serum, we designed and produced a synthetic anti-histone scFv (ahscFv) and a control scFv (cscFv). AhscFv, but not cscFv, recognizes histones H1, H3, and H4 and significantly reduced the toxicity of histones (Figure E2). Similar results were obtained with sera taken from patients with trauma, severe sepsis, and necrotizing pancreatitis (Figure 1F). These data demonstrate that high levels of circulating histones are harmful.

Lungs Are the Most Susceptible Organ to High Levels of Circulating Histones in Mouse Models

After histone infusion, mouse alveolar capillaries became significantly obstructed with neutrophils (12), suggesting that lung injury may have been the cause of death. Using histones at 75 mg/kg, we found that all treated mice developed dyspnea

and cyanosis, a manifestation of pulmonary and cardiac failure, and died within 2 hours. Histological examination showed severe lung edema and multifocal alveolar hemorrhage (Figure 2Ab; and *see* Figure E3a). Pathological changes in other organs, including liver and kidney, were not as obvious as that in the lungs (Figure 2A), except for vacuole formation in some cases (Figures E3e and E3f). Specifically, lung injury was significantly reduced by coinfusion of ahscFv (10 mg/kg), a minimal dose that could rescue all mice challenged with the same dose of histones (Figure 2B; and *see* Figures E2F and E3c).

To demonstrate that endogenous histones are involved in lung injury after trauma, we used the Gierer mouse model of severe trauma (29) and found that high levels of circulating histones appeared 1 hour after trauma (Figure 2C) and reached up to 190 μg/ml after 4 hours. This is similar to observations in trauma patients. Histological examination 4 hours after injury found obvious lung edema, increased alveolar wall thickening, and occasional hemorrhage (Figure 2Db), but these were less severe than that in the histone infusion model. Pathological changes in other organs were not obvious (Figures 2Dc and 2Dd). Coinjection of ahscFv (10 mg/kg) also significantly reduced lung edema (Figures E3b and E3d). Further analysis of blood from these mice did not show severe liver or renal impairment (Figure 2E) although a slight increase in liver enzymes followed histone infusion but not trauma. These data collectively indicate that lungs are much more susceptible to the toxicity of circulating histones than are other organs. This finding supports the clinical observation that lungs are the most commonly affected distant organ and that lung dysfunction precedes that of other organs during MOF development (30). The nature of the pulmonary microcirculation with its dense capillary network (31) organized differently from other organs (32) would be more readily compromised by endothelial damage and coagulation activation.

Postinjury Respiratory Failure Is Associated with Levels of Circulating Histones

In the group of 52 patients with severe nonthoracic blunt trauma, 3 patients died shortly after admission. Of the remaining 49 patients, 19 (39%) developed respiratory failure and their histone levels (median, 52.5 μg/ml; quartiles: 22.1, 76.5) were significantly higher than in patients without respiratory failure (median, 15.6 μg/ml; quartiles: 12.5, 28.5). Among the 17 patients with circulating histones equal to or greater than 50 μg/ml (toxicity threshold, as described previously), 13 (76.5%) developed respiratory failure compared with 6 of 32 patients (18.8%) below this threshold (Fisher exact test, $P = 0.0001$). A simple linear correlation analysis also showed a significant correlation between circulating histone levels and Sequential Organ Failure Assessment (SOFA) scores ($r = 0.55$, $P < 0.01$). These findings suggest that high levels of circulating histones in trauma patients may be prognostic and pathogenic in mediating distant organ damage, especially lung injury and the consequent MOF.

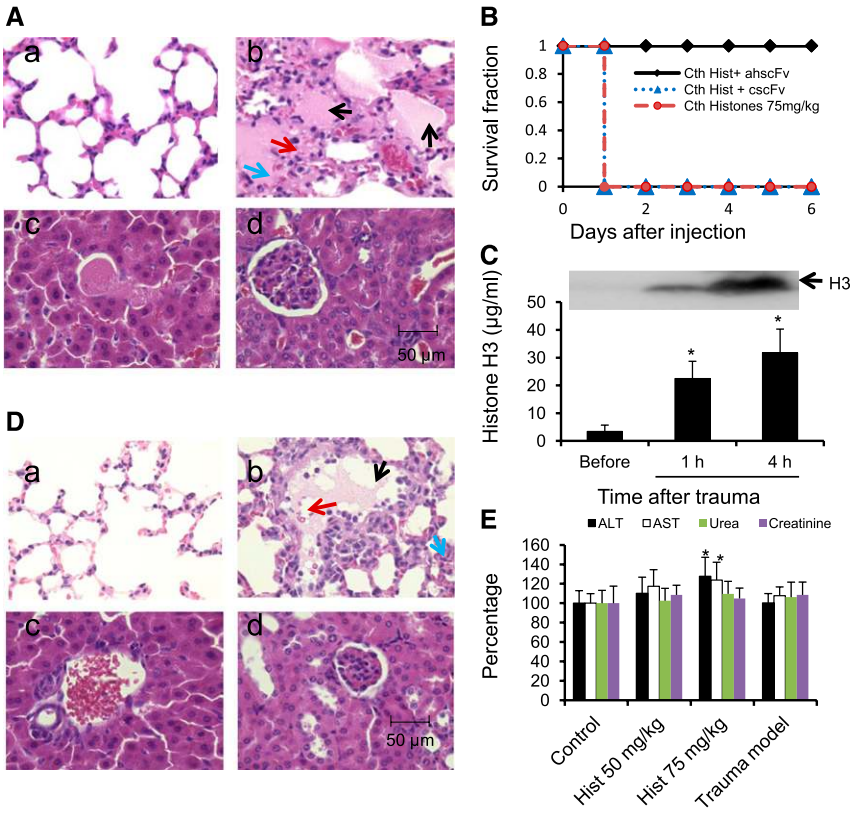

Figure 2. Histone-induced toxicity in mice. (*A*) Hematoxylin and eosin (H&E)-stained sections: (*a*) lung from an untreated mouse and (*b*) lung, (*c*) liver, and (*d*) kidney from a mouse 4 hours after infusion with histones (60 mg/kg). Obvious pathological changes were found in the lungs, such as edema (*black arrows*), microvascular congestion (*red arrow*), and hemorrhage (*blue arrow*) (*b*). Less obvious changes were found in (*c*) the liver and (*d*) kidneys. (*B*) Survival curves of mice injected with calf thymus (Cth) histones (75 mg/kg; a lethal dose) preincubated without (none of seven survived) or with anti-histone scFv (ahscFv, 10 mg/kg) (seven of seven survived) and control scFv (cscFv, 10 mg/ml) (none of seven survived); log-rank test, $P < 0.01$. (*C*) *Top*: An example of histone H3 detected by Western blot in the blood of mice after trauma. *Bottom*: The mean ± SD of circulating histone H3 of 10 mice. *Analysis of variance (ANOVA) test, $P < 0.01$. (*D*) H&E-stained sections: (*a*) lung from an untreated mouse; (*b*) lung, (*c*) liver, and (*d*) kidney, respectively, from a mouse 4 hours after major trauma. Similar but less severe pathological changes than those in *A* were observed, with *arrows* indicating edema (*black*), congestion (*red*), and hemorrhage (*blue*). Scale bar: 50 μm. (*E*) Liver function, as measured by aspartate transaminase (AST) and alanine transaminase (ALT), and renal function, as measured by urea and creatinine, in the blood of untreated mice, mice infused with histone at 50 mg/kg (nonlethal dose) or 75 mg/kg (lethal dose), and mice after severe trauma (10 per group). Blood was taken 4 hours after treatment or just before death in the group infused with a lethal dose of histones. Mean from untreated group was designated as 100% and the relative percentages are presented. *ANOVA test shows a significant increase compared with the untreated group ($P < 0.05$).

Lung Injury Is Associated with Histone-induced Endothelial Damage and Coagulation Activation

Previous reports showed that circulating histones cause mainly endothelial damage (12). To test whether these observations might be relevant to patients with severe blunt trauma, we first examined circulating soluble thrombomodulin (sTM), a marker for endothelial damage (33). sTM was significantly higher in the 52 patients compared with healthy donors (Figure 3A). In mouse models, sTM was elevated immediately after trauma or histone infusion (Figures 3B and 3C). Importantly, sTM was also significantly correlated with circulating histone levels ($r = 0.55$, $P < 0.001$) in trauma patients. In examining further for pathogenic relevance, we observed histone-induced endothelial permeability increase *in vitro* (Figure 3D). Furthermore, the ratio of wet to dry lung weight in mouse models was altered to indicate increased vascular permeability *in vivo* (Figure 3E). These data are consistent with the histological changes observed in mice and previous postmortem finding in trauma patients (5).

Coagulation activation is another major factor of histone toxicity observed *in vitro* and in mice (15, 28). To test whether this occurs in trauma patients, we detected thrombin–anti-thrombin (TAT) complexes, a marker for coagulation activation (34). TAT was significantly increased (Figure 4A) and also correlated with circulating histone levels ($r = 0.56$, $P < 0.001$). In mouse models, TAT was elevated soon after trauma and histone infusion (Figures 4B and 4C). The formation of thrombi in lungs and occasionally in kidneys (Figures 4Db and 4Dd, and 4Ed) strongly supports the contention that histone-triggered coagulation activation is involved in lung injury and possibly MOF.

Major Mechanism of Histone Toxicity Is Calcium Influx Caused by Plasma Membrane Disruption

How histones cause cellular damage is not clear. Histones have been reported to increase membrane permeability in thymocytes (35), transepithelial conductance in rabbit urinary bladder epithelium (36), intracellular calcium elevation in MCF-7 cells (37) and platelets (15, 16, 28), as well as activation of Toll-like receptors (TLRs) (13, 14). Given the apparent susceptibility of various cells to histones, we speculate that the negatively charged phosphate groups in phospholipids could be their target site

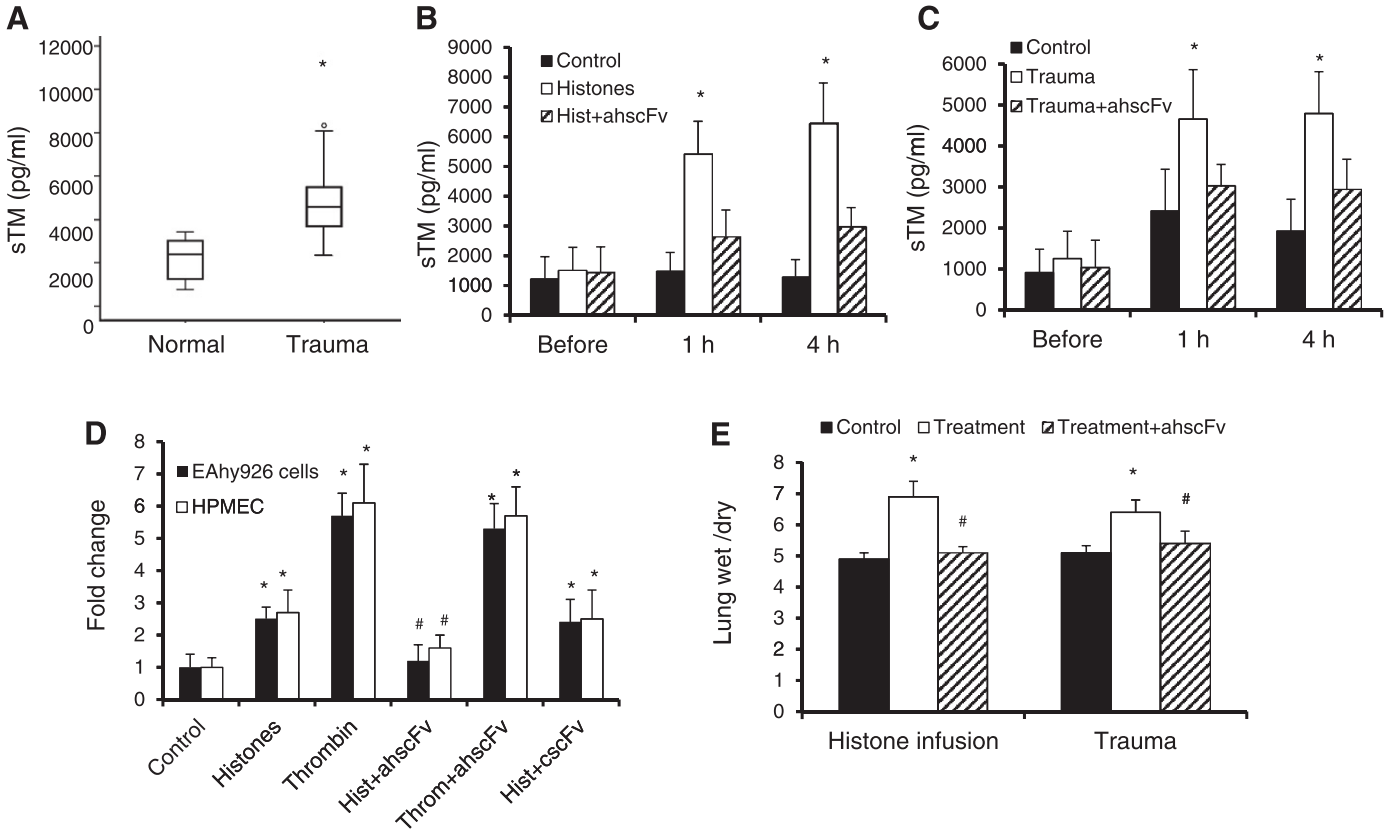

Figure 3. Histone-induced endothelial damage and permeability increase. (*A*) Box plot shows the medians of circulating soluble thrombomodulin (sTM) levels in 20 healthy donors (Normal) and 52 patients with severe nonthoracic trauma. *Median test, $P = 0.01$. (*B*) Mean ± SD of circulating sTM in mice infused with saline (Control), calf thymus histones (Histones, 50 mg/ml; a nonlethal dose) or histones plus anti-histone scFv (10 mg/kg) (Hist+ahscFv) (10 mice per group). *Analysis of variance (ANOVA) test, $P < 0.05$ compared with the Control and Hist+ahscFv groups. (*C*) Mean ± SD of circulating sTM in mice treated with anesthetics alone (Control), mice subjected to trauma (Trauma), and mice infused with ahscFv (10 mg/kg) 10 minutes prior to trauma (Trauma+ahscFv) (10 mice per group). *ANOVA test, $P < 0.05$ compared with Control and Trauma+ahscFv groups of the same time point. (*D*) *In vitro* permeability assay, using Transwells plated with EA.hy926 cells and human pulmonary microvascular endothelial cells (HPMECs; *see* METHODS). Fully confluent monolayers of cells on the membrane of Transwells were treated with histones (50 μg/ml) or 2 units of thrombin preincubated without or with ahscFv (200 μg/ml) or control scFv (cscFv). Fold changes (means ± SD) compared with controls (treated with buffer alone) from five independent experiments are shown. *ANOVA test, $P < 0.05$ compared with control. #Student *t* test shows significant reduction compared with histones alone, $P < 0.05$. (*E*) Means ± SD of right lung wet-to-dry weight ratios (METHODS) of mice 4 hours after infusion with calf thymus histones (60 mg/kg) or trauma models (10 mice per group). *ANOVA test, $P < 0.05$ compared with control (saline infusion or anesthetics alone). #Student *t* test shows significant reduction compared with the treatment group, $P < 0.05$.

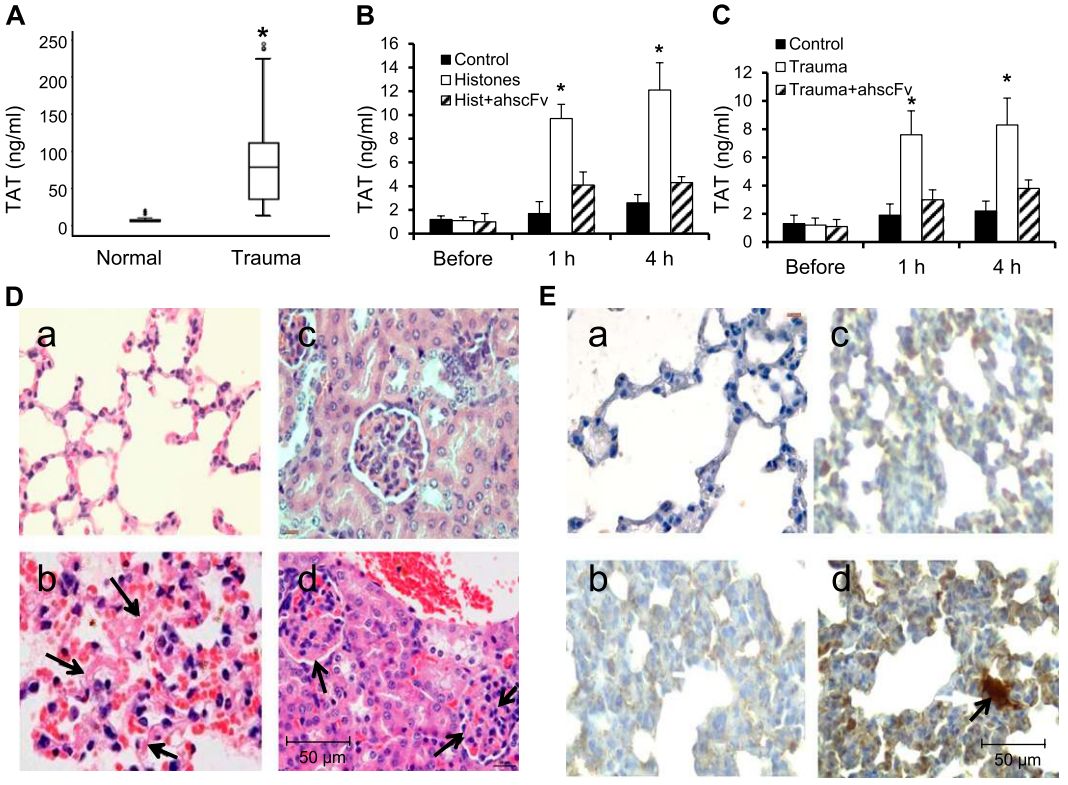

Figure 4. Histone-induced coagulation activation *in vivo*. (*A*) Box plot shows the medians of thrombin–anti-thrombin (TAT) levels in 20 healthy donors (Normal) and 52 patients with severe nonthoracic trauma. *Median test, $P = 0.001$. (*B*) Mean ± SD of TAT in mice infused with saline (Control), calf thymus histones (Histones, 50 mg/ml), or histones plus anti-histone scFv (ahscFv, 10 mg/kg) (Hist+ahscFv) (10 mice per group). *Analysis of variance (ANOVA) test, $P < 0.05$ compared with Control and Hist+ahscFv groups. (*C*) Mean ± SD of TAT in mice treated with anesthetics alone (Control), mice subjected to trauma (Trauma), and mice infused with ahscFv (10 mg/kg) 10 minutes before trauma (Trauma+ahscFv) (10 mice per group). *ANOVA test, $P < 0.05$ compared with Control and Trauma+ahscFv groups. (*D*) Tissue sections from (*a* and *c*) untreated mice and (*b* and *d*) mice infused with a 75-mg/kg concentration of calf thymus histones. (*b*) Hematoxylin and eosin (H&E)–stained lung section with microvascular thrombi (*arrows*). (*d*) H&E-stained kidney section with thrombi (*arrow*). (*E*) Immunohistochemical staining of lung sections from (*a*) an untreated mouse and (*b–d*) mice after infusion of histones (75 mg/kg). (*a* and *d*) Stained with anti-fibrin; (*b*) stained with secondary antibody only; (*c*) probed with anti-fibrin preincubated with fibrin (Sigma) as controls. *Arrow* in *d* indicates thrombosis in an anti-fibrin–stained lung section. Scale bars: 50 μm.

because in nucleosomes, the histone core interacts with the phosphodiester bonds of DNA, as resolved by crystallography (38). Phospholipids, the main structural components of plasma membranes, also possess phosphodiester bonds and have been shown to interact with histones (39). We found that fluorescein isothiocyanate (FITC)–labeled histones in culture medium started to outline endothelial cell membranes after a 10-minute incubation (Figure 5A, *left*), which could be blocked by preincubation with ahscFv (Figure 5A, *right*). FITC-labeled bovine serum albumin did not outline any of the cell membrane (data not shown). In mice, histone infusion generates histone staining on endothelial cell membrane surfaces (Figure 5B, *left*) but not in untreated mice (Figure 5B, *right*). These results clearly demonstrate the membrane-binding property of extracellular histones. Using the perforated patch configuration from single EA.hy926 cells, as previously described (23), whole-cell currents were recorded immediately after histone binding (Figure 5C). Intracellular Ca^{2+} was elevated after exposure to histones (Figure 5D), which was abolished when extracellular Ca^{2+} was removed (Figure 5E), indicating Ca^{2+} influx as a major cause. By controlling extracellular Ca^{2+}, we found that it is essential for histone-induced cell damage (Figure 5F). TLR4- and TLR2-neutralizing antibodies did not block the calcium influx and showed no protective effect on cultured endothelial cells treated with histones (Figure E4A). This suggests that activation of these receptors is not the major pathway for histone toxicity, at least in endothelial cells.

Direct Effects of Histones on Leukocytes Contribute to the Heightened Postinjury Inflammatory State

Besides endothelial damage and coagulation activation, the cytokine surge and neutrophil activation are central players in trauma-associated lung injury and MOF, based on current theories. It is hypothesized that increased gut permeability allows endotoxin or bacteria to enter the circulation, which triggers cytokine release and primes neutrophils (7, 8). Activated neutrophils would then release toxic mediators, including reactive oxygen species (ROS) and MPO to damage lungs and other organs (7). However, the links in this pathway have never been clearly demonstrated. It was found that cytokines, including tumor necrosis factor-α, IL-6, and IL-10 are elevated in mice 2 hours after exogenous histone infusion (13), and IL-6 mRNA synthesis was increased in hepatocytes (14). However, newly synthesized IL-6 mRNA will take a few hours before IL-6 protein reaches significantly high levels in the circulation. In fact, the IL-6 surge occurred within 2 hours in previous reports (40), within 4 hours in our cohort of trauma patients (data not shown), and as early as 1 hour in mice after trauma or histone infusion (Figure 6A). Therefore, IL-6 is most likely to be released from presynthesized storage. Using flow cytometry, we found that IL-6 exists within leukocytes, including lymphocytes, neutrophils, and monocytes, from healthy donors (Figure 6B) and was released on stimulation with histones at concentrations as low as 20 μg/ml (Figure 6C) within 2 hours (Figure 6D), without significant increases in IL-6 mRNA (data not shown). Anti-TLR4 at high concentration (20 μg/ml), but not anti-TLR2 partially reduced IL-6 release by 20–30% (Figure E4B). In contrast, IL-6 release strongly relied on influx of extracellular calcium (Figure 6E). The IL-6 release was not due to LPS contamination (Figure E5) and was inhibited by ahscFv from both isolated leukocytes (Figure 6D) and in mouse models (Figure 6A). More importantly, IL-6 levels in patients significantly correlated with circulating histones ($r = 0.55$, $P < 0.01$). These findings demonstrate that the early cytokine surge in trauma

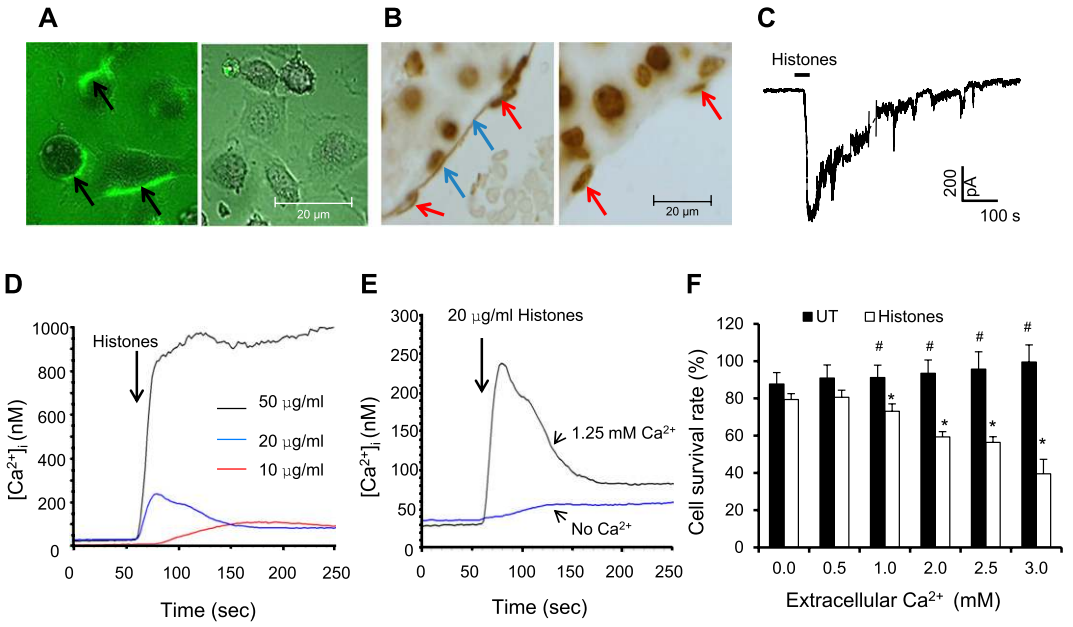

Figure 5. Membrane binding and calcium influx determine histone toxicity in endothelial cells. (*A*) Confocal images of EA.hy926 cells 10 minutes after incubation with fluorescein isothiocyanate (FITC)–labeled histones (10 μg/ml) alone (*left*) or FITC-labeled histones preincubated with anti-histone scFv (ahscFv; 100 μg/ml) (*right*). *Arrows* indicate the membrane associated with FITC-labeled histones. Scale bar: 20 μm. (*B*) Immunohistochemical staining of histone H3 in tissues from a mouse 4 hours after infusion with histones at 60 mg/kg (*left*) and an untreated mouse (*right*). *Red arrows* indicate endothelial nuclei and *blue arrows* point to a continuous line between endothelial nuclei stained with anti-histones to indicate association of histones with the plasma membranes of endothelial cells. Scale bar: 20 μm. (*C*) Representative whole-cell currents recorded from EA.hy926 cells when histones (20 μg/ml) were applied to the extracellular bathing solution. Currents generated by application of histones were reversible by washing after a short exposure (30–60 s). (*D*) Example of elevation of intracellular Ca^{2+} recorded with a Hitachi F-7000 fluorescence spectrometer when EA.hy926 cells were exposed to various histone concentrations. (*E*) Example of intracellular Ca^{2+} elevation triggered by histones (20 μg/ml) that was nearly abolished by removal of Ca^{2+} from extracellular medium. (*F*) Survival rates (mean ± SD) of cells incubated for 1 hour with medium containing 0–3 mM Ca^{2+} in the presence or absence of histones (20 μg/ml), from three independent experiments. *Significant reduction in cell survival rate compared with that without Ca^{2+} (analysis of variance test, $P < 0.05$). #Student *t* test shows significantly higher survival rates than when treated with histones ($P < 0.05$).

patients is due mainly to histone-induced release of prestored cytokines from leukocytes and that circulating histones are major mediators of the high inflammatory states after severe blunt trauma.

Histone-induced MPO Release and NET Formation May Contribute to Cell Damage, Lung Capillary Congestion, and Thrombosis

Neutrophil congestion inside the capillaries of lungs in mice treated with histones was reported by Xu and colleagues (12). We also found pulmonary capillary congestion and significant neutrophil infiltration in the lungs of our mouse models by anti-MPO immunohistochemical staining (Figure 7A, *left*). As neutrophil activation is considered to be a major mechanism for lung injury after severe trauma, we further examined whether histones could stimulate neutrophils to release these toxic mediators, such as ROS (41) and MPO (42). In mice infused with histones, MPO staining was found inside alveoli (Figure 7A, *right*), indicating MPO was released on histone infusion. Using isolated neutrophils, we found that histones, unlike phorbol myristate acetate (PMA), were unable to induce ROS production (data not shown) but caused significant MPO release (Figure 7B). Because MPO enhances the production of hypochlorous acid from hydrogen peroxide and chloride anion, which kills bacteria but also damages host cells, increased MPO release may further contribute to lung injury, including alveolar epithelial cell damage.

How neutrophils are trapped in lung capillaries is not clear, although damaged endothelium and cytokine-primed neutrophils may contribute to the congestion. We tested whether histones could directly cause morphological changes in neutrophils and found that histones, like PMA, induced the formation of neutrophil extracellular trap (NET)–like structures (Figure 7C, *left*). Histones at 50 μg/ml induced a percentage of NET-like structures similar to that induced by PMA within a 3-hour incubation (Figure 7C, *right*; and *see* Figure E6). Citrullinated histone H3 (CitH3), a marker for NETs (43–45), was positive in the lungs of mice injected with histones (Figure 7D; and *see* Figure E7), and coinfusion with ahscFv significantly reduced the number of anti-CitH3–stained cells (Figure E8). These data suggest that NET formation may serve as a mechanism for neutrophil congestion and thrombosis in lungs.

DISCUSSION

Our work has demonstrated that circulating histones are able to mediate distant organ damage, particularly of the lungs, and contribute to MOF. We believe that these findings significantly advance understanding of this common and frequently life-threatening clinical syndrome while also clarifying and resolving the discrepancies within current theories in this field. Of important translational relevance is a real prospect for clinical management of patients after severe blunt trauma to improve with development of antihistone therapeutics.

Extracellular histones bind phospholipids, disrupt cell membranes, and cause calcium influx. This indiscriminate activity on all cells tested results in sustained elevation of $[Ca^{2+}]_i$ causing cell damage (46) and release of cellular stores and content. Included in this is inflammatory cytokines, for example, IL-6, which we demonstrate to be presynthesized within leukocytes. This is a generic mechanism that is not cell type or species specific (Figures E1D and E1E), although TLR4 can be partially responsible for cytokine release (Figure E4B). Importantly, this finding now provides a credible explanation for the early cytokine surge and enhanced inflammatory state after

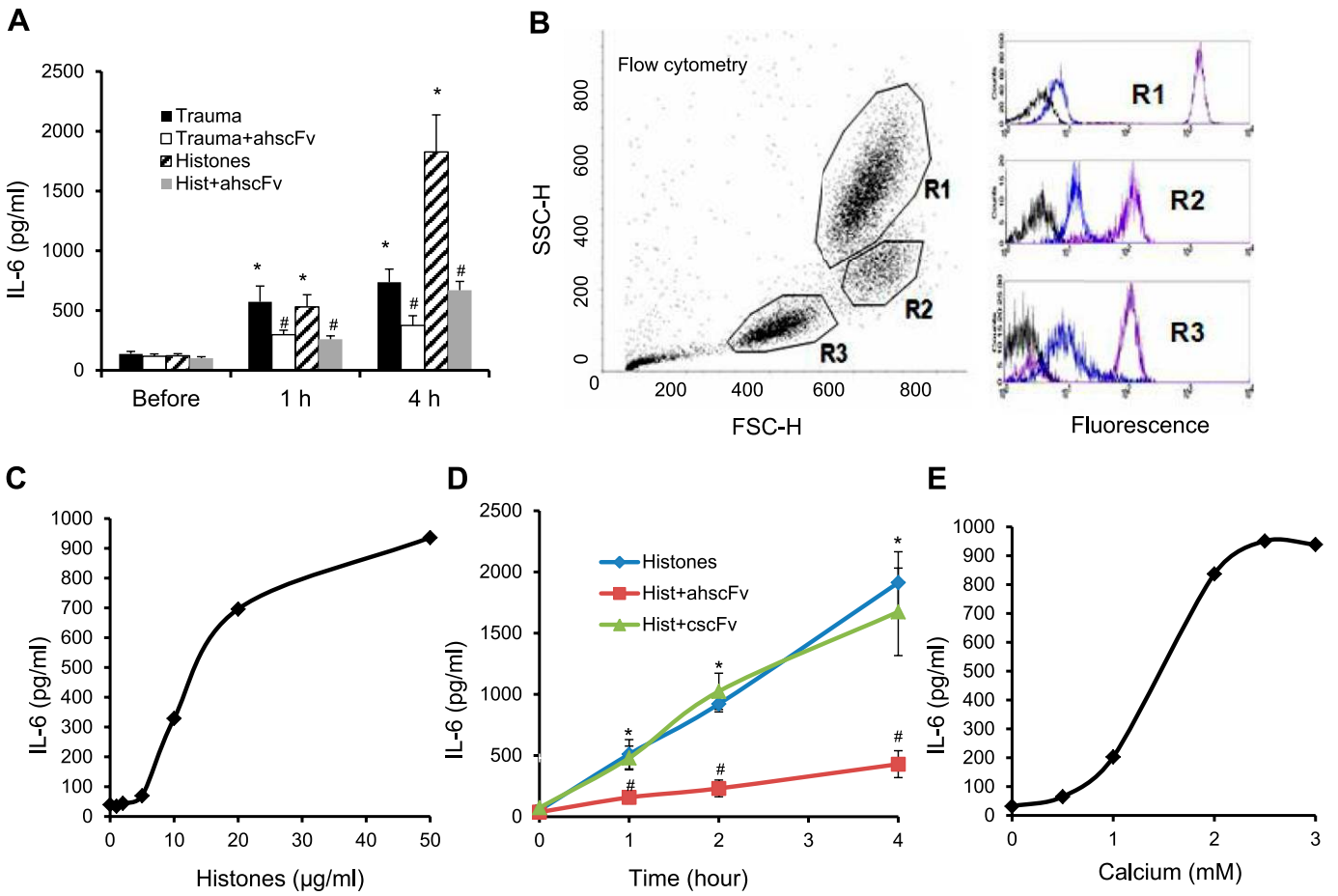

Figure 6. Histone-triggered cytokine release. (*A*) Circulating IL-6 levels in both the mouse trauma model (Trauma) and the histone infusion model with or without the coinfusion of anti-histone scFv (ahscFv, 10 mg/kg). With 10 mice per group, the means ± SD of IL-6 are shown. *Analysis of variance (ANOVA) test shows a significant increase compared with that before treatment (Before), $P < 0.01$. #Student *t* test shows significant reduction compared with that without ahscFv coinfusion, $P < 0.05$. (*B*) *Left*: Direct flow cytometric analysis of human leukocytes from healthy donors. R1 = neutrophils; R2 = monocytes; R3 = lymphocytes. *Right*: Flow cytometric analysis of the same sample but fluorescently stained with rat IgG–phycoerythrin (PE) (*black*), rat anti-human IL-6–PE (*blue*), anti-CDs–fluorescein isothiocyanate (FITC) (*purple*) (R1, CD15 for neutrophils; R2, CD14 for monocytes; and R3, CD3 for lymphocytes) to demonstrate the storage of presynthesized IL-6 in peripheral leukocytes from healthy donors. (*C*) IL-6 release from freshly isolated leukocytes incubated with various histone concentrations for 2 hours. A typical dose–response curve is shown. (*D*) Isolated leukocytes were incubated with histones (50 μg/ml) in the absence (*blue*) or presence of ahscFv (200 μg/ml) (*red*) and control scFv (cscFv) (*green*). The supernatants were collected at various time points for determination of IL-6 concentration. A time course of means ± SD is shown from three repeats. *ANOVA test shows significant increase compared with time zero ($P < 0.05$). #ANOVA test shows significant reduction compared with the same time point but without ahscFv ($P < 0.05$). (*E*) Extracellular Ca^{2+} effects on IL-6 release from leukocytes treated with histones (50 μg/ml) for 2 hours. A typical dose–response curve is shown.

trauma that has long been implicated in the pathogenesis of MOF. Although the gut hypothesis may be relevant in simple hemorrhagic shock (47), it hardly explains why these cytokines surge abruptly within 2 hours in trauma patients without shock and in mice from as early as 1 hour after injury.

Cytokine priming and activation of neutrophils are considered a major cause of secondary lung injury after trauma (42). Lung capillaries congested with neutrophils were observed by Xu and colleagues (12). However, histone-induced NET formation may increase the chance of neutrophils being trapped, together with other blood cells, to facilitate thrombosis (48). As NETs also release histones and directly induce surrounding cell death (49), histone-induced NETs may well contribute to a vicious cycle that further enhances lung injury. Although histones do not directly stimulate ROS production, significant MPO release was induced, which may also amplify this inflammatory injury. Nonetheless, these mechanisms would not exclude the possible role of endotoxins or bacteria from gut hyperpermeability at later stages. It therefore remains likely that the multihit theory may best describe the whole process of trauma-associated MOF (50), but the role of circulating histones within the first hit would appear to be significant and potentially targetable for lung injury after severe nonthoracic trauma.

In conclusion, our results show that circulating histones play a major clinical and pathological role in trauma-associated lung injury and possibly MOF, with the mechanisms summarized in Figure E9. Besides trauma, extensive cell death occurs in the acute phase of many human diseases, and we found histone-specific cytotoxic effects in the sera of patients with sepsis and necrotizing pancreatitis. Lung dysfunction and MOF are common in these diseases, and circulating histones may also play an important role. Future translational intervention with assays to monitor circulating histone levels and

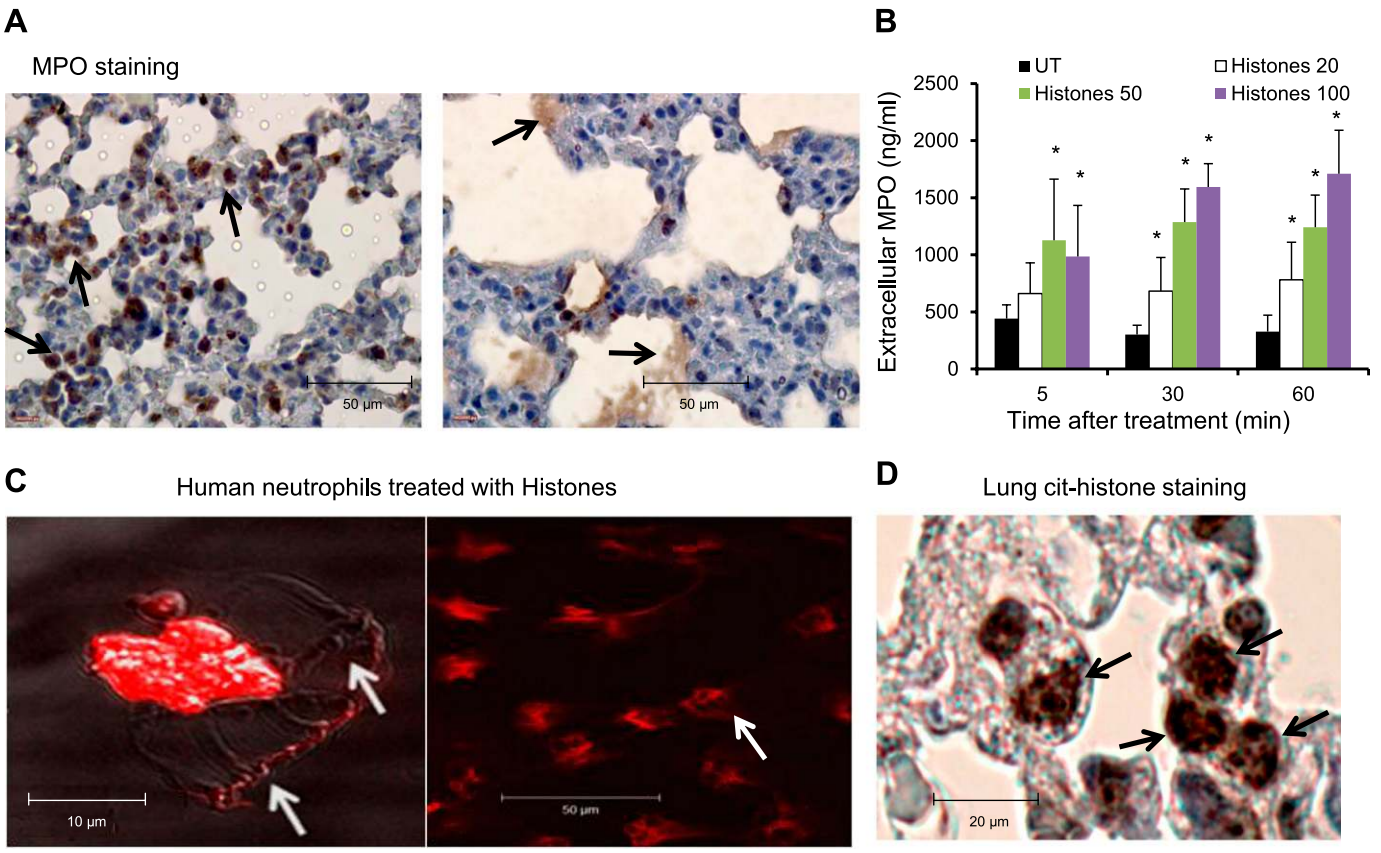

Figure 7. Effects of histones on neutrophils. (*A*) Anti-myeloperoxidase (MPO)–stained lung sections. *Left*: A mouse with trauma shows MPO-positive cell infiltration (*arrows*). *Right*: A mouse infused with calf thymus histones (60 mg/kg) shows MPO inside alveoli (*arrows*), a possible neutrophil breakdown product. Scale bar: 50 μm. (*B*) Increased release of MPO from isolated human neutrophil after histone treatment (METHODS). The means ± SD of extracellular MPO from three independent experiments are shown. *Analysis of variance test shows a significant increase compared with untreated (UT), $P < 0.05$. (*C*) Neutrophil extracellular trap (NET) formation after treatment with histone at 50 mg/ml (METHODS). *Left*: A typical NET-like structure stained with propidium iodide (*red*). *Arrows* indicate that DNA fibers are outside the cell nucleus. Scale bar: 10 μm. *Right*: Most cells develop NET-like structures after 3 hours of histone treatment. Scale bar: 50 μm. (*D*) Anti–citrullinated (cit)-histone–stained lung section from a mouse infused with histones (60 mg/kg). *Arrows* indicate cit-histone–positive neutrophils congested inside alveolar walls. Scale bar: 20 μm.

antihistone therapies could be highly relevant in reducing lung injury and MOF to improve overall outcome in many critical illnesses.

Author disclosures are available with the text of this article at www.atsjournals.org.

Acknowledgment: The authors are indebted to participating patients and their attending clinical staff. J.M. has a research fellowship from the Royal College of Surgeons, England. The authors also acknowledge the National Institute of Health Research (NIHR Biomedical Research Centre in Microbial Disease Grant Project [3515] and NIHR Innovation for Invention Grant [II-LS-1010-14061]) for infrastructural and project support.

References

1. Gomberg BF, Gruen GS, Smith WR, Spott M. Outcomes in acute orthopaedic trauma: a review of 130,506 patients by age. *Injury* 1999;30:431–437.
2. Dewar D, Moore FA, Moore EE, Balogh Z. Postinjury multiple organ failure. *Injury* 2009;40:912–918.
3. Tsukamoto T, Chanthaphavong RS, Pape HC. Current theories on the pathophysiology of multiple organ failure after trauma. *Injury* 2010; 41:21–26.
4. Ciesla DJ, Moore EE, Johnson JL, Burch JM, Cothren CC, Sauaia A. The role of the lung in postinjury multiple organ failure. *Surgery* 2005; 138:749–757; discussion 757–748.
5. Martin AM Jr, Soloway HB, Simmons RL. Pathologic anatomy of the lungs following shock and trauma. *J Trauma* 1968;8:687–699.
6. Zallen G, Moore EE, Johnson JL, Tamura DY, Aiboshi J, Biffl WL, Silliman CC. Circulating postinjury neutrophils are primed for the release of proinflammatory cytokines. *J Trauma* 1999;46:42–48.
7. Swank GM, Deitch EA. Role of the gut in multiple organ failure: bacterial translocation and permeability changes. *World J Surg* 1996;20: 411–417.
8. Moore FA. The role of the gastrointestinal tract in postinjury multiple organ failure. *Am J Surg* 1999;178:449–453.
9. Peltz ED, Moore EE, Eckels PC, Damle SS, Tsuruta Y, Johnson JL, Sauaia A, Silliman CC, Banerjee A, Abraham E. HMGB1 is markedly elevated within 6 hours of mechanical trauma in humans. *Shock* 2009;32:17–22.
10. Holdenrieder S, Stieber P. Clinical use of circulating nucleosomes. *Crit Rev Clin Lab Sci* 2009;46:1–24.
11. Gauthier VJ, Tyler LN, Mannik M. Blood clearance kinetics and liver uptake of mononucleosomes in mice. *J Immunol* 1996;156:1151–1156.
12. Xu J, Zhang X, Pelayo R, Monestier M, Ammollo CT, Semeraro F, Taylor FB, Esmon NL, Lupu F, Esmon CT. Extracellular histones are major mediators of death in sepsis. *Nat Med* 2009;15:1318–1321.
13. Xu J, Zhang X, Monestier M, Esmon NL, Esmon CT. Extracellular histones are mediators of death through TLR2 and TLR4 in mouse fatal liver injury. *J Immunol* 2011;187:2626–2631.
14. Huang H, Evankovich J, Yan W, Nace G, Zhang L, Ross M, Liao X, Billiar T, Xu J, Esmon CT, *et al*. Endogenous histones function as alarmins in sterile inflammatory liver injury through Toll-like receptor 9 in mice. *Hepatology* 2011;54:999–1008.

15. Fuchs TA, Bhandari AA, Wagner DD. Histones induce rapid and profound thrombocytopenia in mice. *Blood* 2011;118:3708–3714.
16. Ammollo CT, Semeraro F, Xu J, Esmon NL, Esmon CT. Extracellular histones increase plasma thrombin generation by impairing thrombomodulin-dependent protein C activation. *J Thromb Haemost* 2011;9:1795–1803.
17. Wang G. Anti-histone scFv protects endothelial cells from the toxicity of circulating histones [abstract]. Paper presented at the 4th Annual international Congress of Antibodies (ICA-2012). Beijing, China, March 26–28, 2012.
18. Shechter D, Dormann HL, Allis CD, Hake SB. Extraction, purification and analysis of histones. *Nat Protoc* 2007;2:1445–1457.
19. Monestier M, Fasy TM, Losman MJ, Novick KE, Muller S. Structure and binding properties of monoclonal antibodies to core histones from autoimmune mice. *Mol Immunol* 1993;30:1069–1075.
20. Riccardi C, Nicoletti I. Analysis of apoptosis by propidium iodide staining and flow cytometry. *Nat Protoc* 2006;1:1458–1461.
21. Perez-Casal M, Downey C, Cutillas-Moreno B, Zuzel M, Fukudome K, Toh CH. Microparticle-associated endothelial protein C receptor and the induction of cytoprotective and anti-inflammatory effects. *Haematologica* 2009;94:387–394.
22. Becker PM, Kazi AA, Wadgaonkar R, Pearse DB, Kwiatkowski D, Garcia JG. Pulmonary vascular permeability and ischemic injury in gelsolin-deficient mice. *Am J Respir Cell Mol Biol* 2003;28:478–484.
23. Leyland ML, Dart C. An alternatively spliced isoform of PSD-93/chapsyn 110 binds to the inwardly rectifying potassium channel, Kir2.1. *J Biol Chem* 2004;279:43427–43436.
24. Grynkiewicz G, Poenie M, Tsien RY. A new generation of Ca^{2+} indicators with greatly improved fluorescence properties. *J Biol Chem* 1985;260:3440–3450.
25. Holdenrieder S, Stieber P, Bodenmuller H, Busch M, Von Pawel J, Schalhorn A, Nagel D, Seidel D. Circulating nucleosomes in serum. *Ann N Y Acad Sci* 2001;945:93–102.
26. Baker SP, O'Neill B, Haddon W Jr, Long WB. The injury severity score: a method for describing patients with multiple injuries and evaluating emergency care. *J Trauma* 1974;14:187–196.
27. Pemberton AD, Brown JK, Inglis NF. Proteomic identification of interactions between histones and plasma proteins: implications for cytoprotection. *Proteomics* 2010;10:1484–1493.
28. Semeraro F, Ammollo CT, Morrissey JH, Dale GL, Friese P, Esmon NL, Esmon CT. Extracellular histones promote thrombin generation through platelet-dependent mechanisms: involvement of platelet TLR2 and TLR4. *Blood* 2011;118:1952–1961.
29. Gierer P, Hoffmann JN, Mahr F, Menger MD, Mittlmeier T, Gradl G, Vollmar B. Sublethal trauma model with systemic endotoxemia for the study of microcirculatory disorders after the second hit. *J Surg Res* 2008;147:68–74.
30. Slutsky AS, Tremblay LN. Multiple system organ failure: is mechanical ventilation a contributing factor? *Am J Respir Crit Care Med* 1998; 157:1721–1725.
31. Gil J. Organization of microcirculation in the lung. *Annu Rev Physiol* 1980;42:177–186.
32. Gil J. Microcirculation of the lung: functional and anatomic aspects. In: Yuan J, editor. Textbook of pulmonary vascular disease. New York: Springer Science+Business Media; 2011. pp. 13–24.
33. Constans J, Conri C. Circulating markers of endothelial function in cardiovascular disease. *Clin Chim Acta* 2006;368:33–47.
34. Haaland AK, Skjonsberg OH, Gravem K, Ruyter R, Godal HC. Comparison of thrombin–antithrombin complex (TAT) levels and fibrinopeptide A following thrombin incubation of human plasma using hirudin as an inhibitor of Tat formation. *Thromb Res* 1991;61:253–259.
35. Abakushin DN, Zamulaeva IA, Poverenny AM. Histones evoke thymocyte death *in vitro*; histone-binding immunoglobulins decrease their cytotoxicity. *Biochemistry (Mosc)* 1999;64:693–698.
36. Kleine TJ, Lewis PN, Lewis SA. Histone-induced damage of a mammalian epithelium: the role of protein and membrane structure. *Am J Physiol* 1997;273:C1925–C1936.
37. Ganapathy V, Shyamala CS. Effect of histone H1 on the cytosolic calcium levels in human breast cancer MCF 7 cells. *Life Sci* 2005;76: 2631–2641.
38. Luger K, Mader AW, Richmond RK, Sargent DF, Richmond TJ. Crystal structure of the nucleosome core particle at 2.8 Å resolution. *Nature* 1997;389:251–260.
39. Pereira LF, Marco FM, Boimorto R, Caturla A, Bustos A, De la Concha EG, Subiza JL. Histones interact with anionic phospholipids with high avidity; its relevance for the binding of histone–antihistone immune complexes. *Clin Exp Immunol* 1994;97:175–180.
40. Jawa RS, Anillo S, Huntoon K, Baumann H, Kulaylat M. Interleukin-6 in surgery, trauma, and critical care. II. Clinical implications. *J Intensive Care Med* 2011;26:73–87.
41. Partrick DA, Moore FA, Moore EE, Barnett CC Jr, Silliman CC. Neutrophil priming and activation in the pathogenesis of postinjury multiple organ failure. *New Horiz* 1996;4:194–210.
42. Perl M, Hohmann C, Denk S, Kellermann P, Lu D, Braumuller S, Bachem MG, Thomas J, Knoferl MW, Ayala A, *et al*. Role of activated neutrophils in chest trauma–induced septic acute lung injury. *Shock* 2012;38:98–106.
43. Li Y, Liu B, Fukudome EY, Lu J, Chong W, Jin G, Liu Z, Velmahos GC, Demoya M, King DR, *et al*. Identification of citrullinated histone H3 as a potential serum protein biomarker in a lethal model of lipopolysaccharide-induced shock. *Surgery* 2011;150:442–451.
44. Brill A, Fuchs TA, Savchenko AS, Thomas GM, Martinod K, De Meyer SF, Bhandari AA, Wagner DD. Neutrophil extracellular traps promote deep vein thrombosis in mice. *J Thromb Haemost* 2012;10:136–144.
45. Li P, Li M, Lindberg MR, Kennett MJ, Xiong N, Wang Y. PAD4 is essential for antibacterial innate immunity mediated by neutrophil extracellular traps. *J Exp Med* 2010;207:1853–1862.
46. Orrenius S, Nicotera P. The calcium ion and cell death. *J Neural Transm Suppl* 1994;43:1–11.
47. Reino DC, Pisarenko V, Palange D, Doucet D, Bonitz RP, Lu Q, Colorado I, Sheth SU, Chandler B, Kannan KB, *et al*. Trauma hemorrhagic shock-induced lung injury involves a gut-lymph-induced TLR4 pathway in mice. *PLoS One* 2011;6:e14829.
48. Fuchs TA, Brill A, Duerschmied D, Schatzberg D, Monestier M, Myers DD Jr, Wrobleski SK, Wakefield TW, Hartwig JH, Wagner DD. Extracellular DNA traps promote thrombosis. *Proc Natl Acad Sci USA* 2010;107:15880–15885.
49. Saffarzadeh M, Juenemann C, Queisser MA, Lochnit G, Barreto G, Galuska SP, Lohmeyer J, Preissner KT. Neutrophil extracellular traps directly induce epithelial and endothelial cell death: a predominant role of histones. *PLoS One* 2012;7:e32366.
50. Moore EE, Moore FA, Harken AH, Johnson JL, Ciesla D, Banerjee A. The two-event construct of postinjury multiple organ failure. *Shock* 2005;24:71–74.